Molecular engineering of hybrid sensitizers incorporating an organic antenna into ruthenium complex and their application in solar cells

Hyunbong Choi,[a] Chul Baik,[a] Sanghoon Kim,[a] Moon-Sung Kang,[b] Xiang Xu,[de] Hong Seok Kang,[d] Sang Ook Kang,[a] Jaejung Ko,*[a] Md. K. Nazeeruddin*[c] and Michael Grätzel[c]

Received (in Montpellier, France) 18th June 2008, Accepted 15th July 2008
First published as an Advance Article on the web 8th September 2008
DOI: 10.1039/b810332a

Two novel hybrid sensitizers incorporating an organic antenna into a ruthenium complex have been synthesized and applied successfully in nanocrystalline TiO_2 based solar cells, which yielded solar to electricity conversion efficiencies of 8.20–9.16% under AM 1.5 sunlight.

Introduction

Dye-sensitized solar cells (DSSCs) based on nanocrystalline semiconductors have been intensively studied because of their potential low-cost, easy processing and high performance.[1] In these cells, the photo-excitation of the metal-to-ligand charge transfer of the adsorbed sensitizer leads to injection of electrons into the conduction band of the oxide. The oxidized dye is subsequently reduced by electron donation from an electrolyte containing a redox system. The injected electrons flow through the semiconductor network to arrive at the back contact and then through the external load to the counter electrode where they regenerate the hole conductor or redox electrolyte. With a closed external circuit and under illumination, the device then constitutes a photovoltaic energy conversion system, which is regenerative and stable. In this technology, ruthenium complexes have maintained a clear lead in performance amongst thousands of dyes that have been scrutinized resulting the best power conversion efficiencies of 10–11% in standard global air mass 1.5 sunlight.[2] In spite of this, the main drawbacks of ruthenium sensitizers are the lack of absorption in the red region of the visible spectrum and the low molar extinction coefficient. One of the approaches to address these issues would be to incorporate an antenna chromophore into a ruthenium polypyridyl sensitizer. Various groups have investigated antenna-sensitizer assembly to increase the light harvesting efficiency in the spectral sensitization of wide-band gap semiconductors with limited success.[3] In this paper we report meticulously designed antenna ruthenium sensitizers that harvest light efficiently between 400 and 500 nm where the ruthenium sensitizers show large absorption resulting enhanced molar extinction coefficient, and panchromatic response of the hybrid sensitizer.

Results and discussion

Scheme 1 shows structures of the two novel sensitizers **JK-55** and **JK-56**. As an antenna unit, we introduced highly efficient organic systems containing the bis-dimethylfluorenyl amino benzo[*b*]-thiophene donor unit.[4] The ligand, 4,4′-di{bis[(9,9-dimethylfluoren-2-yl)amino]-2-benzo[*b*]thiophenylvinylene}-2,2′-bipyridine, was prepared from 6-[bis(9,9-dimethylfluoren-2-yl)amino]-2-formylbenzo[*b*]thiophene and 4,4′-bis(diethylphosphonomethyl)-2,2′-bipyridine using the Horner–Emmons–Wadsworth reaction.[5] The one-pot synthetic procedure[6] developed for heteroleptic polypyridyl ruthenium sensitizers was adapted for the preparation of two new sensitizers (Scheme 2).

Fig. 1 shows the absorption spectra of **JK-55** and **JK-56** in DMF solution, and absorbed onto thin 4 μm TiO_2 film. The spectrum of **JK-55** displays three absorption peaks at 354, 470 and 539 nm in the visible region. Based on ruthenium sensitizers, the two peaks at 354 and 539 nm are assigned as metal to ligand charge transfer transitions (MLCT). The strong absorption peak at 470 nm is due to the π–π* transition of the incorporated antenna unit. It is interesting to note that the absorbance of **JK-55** and **JK-56** is the exact sum of each constituent unit. The low energy metal-to-ligand charge transfer transition (MLCT) absorption band at 539 nm of **JK-55** sensitizer exhibits a molar extinction coefficient of 22.8 × 10^3 M^{-1} cm^{-1}, which is significantly higher than that of

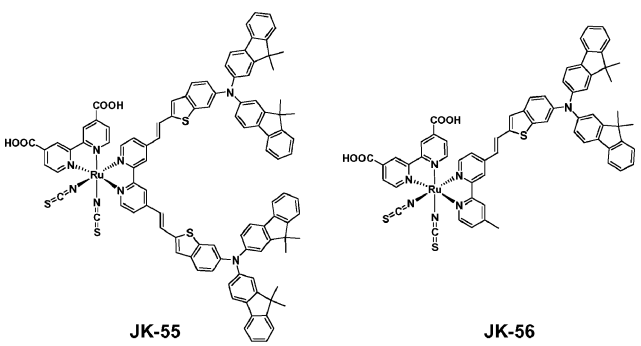

Scheme 1

[a] *Department of New Material Chemistry, Korea University, Jochiwon, Chungnam, 339-700, Korea. E-mail: jko@korea.ac.kr; Fax: 82 41 867 5396; Tel: 82 41 860 1337*
[b] *Energy & Environment Lab. Samsung Advanced Institute of Technology (SAIT) Yongin, 446-712, Korea*
[c] *LPI, Institut des Sciences et Ingénierie Chimiques Faculté des Sciences de Base École Polytechnique Fédérale de Lausanne 1015 Lausanne, Switzerland*
[d] *Department of Nano and Advanced Materials, College of Engineering, Jeonju University, Jeonju, Korea*
[e] *Pohl Institute of Solid State Physics, Tongji University, Shanghai, 200092, P. R. China*

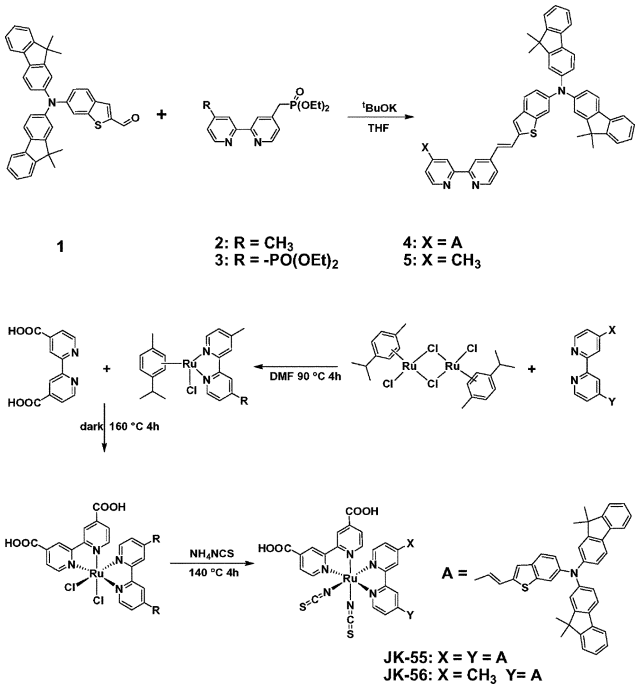

Scheme 2 Schematic diagram for the synthesis of **JK-55** and **JK-56**.

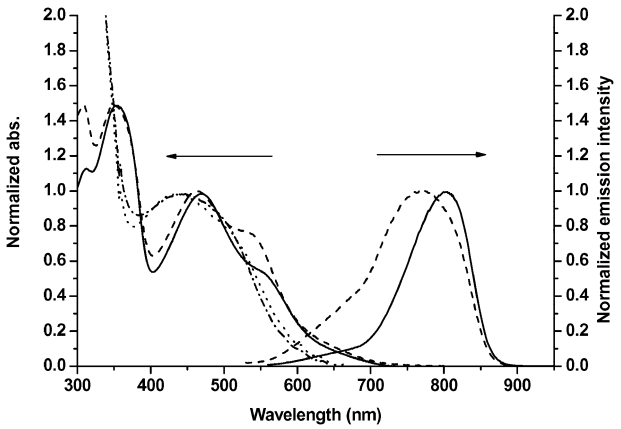

Fig. 1 Absorption and emission spectra of **JK-55** (—) and **JK-56** (--) in DMF and absorption spectra of **JK-55** (···) and **JK-56** (-·-) absorbed onto (4 μm) TiO_2 film. The emission spectra were obtained by exciting at 520 nm for **JK-55** and **JK-56** at 298 K.

N719 dye (14.7×10^3 M^{-1} cm^{-1}). The enhanced molar extinction coefficient, and the red shift is due to the extension of the π-conjugation in the hybrid sensitizer.

Molecular-orbital calculations illustrate that the HOMO of **JK-55** is localized over the NCS unit through benzo[*b*]-thiophene and the LUMO is localized over the 4,4′-dicarboxy-2,2′-bipyridne (Fig. 2). The HOMO−1 for the **JK-55** is shifted to the secondary electron donor moiety, displacing the positive charge (hole) in the oxidized form of **JK-55** from NCS ligands through the fluorenylamino unit. This results in an increased separation of the HOMO−1 orbital from the TiO_2 surface, as desired in order to achieve slower charge-recombination dynamics. Examination of the HOMO and LUMO of two sensitizers indicates that HOMO–LUMO excitation moved the electron distribution from the NCS unit

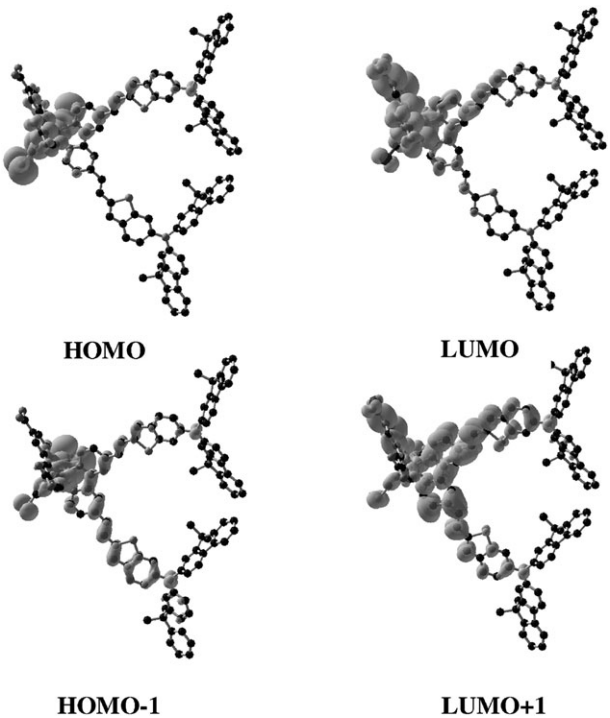

Fig. 2 Isodensity surface plots of the HOMO, HOMO−1, LUMO and LUMO + 1 of **JK-55**.

to the 4,4′-dicarboxy-2,2′-bipyridine ligand and the photo-induced electron transfer from the dye to TiO_2 electrode can be efficiently mediated by the HOMO–LUMO transition.

The cyclic voltammograms of **JK-55** and **JK-56** on TiO_2 films in CH_3CN with 0.1 M tetrabutylammonium hexafluorophosphate show quasi-reversible couples at 1.02 and 1.05 V *vs.* NHE, respectively (Fig. 3). The ground state redox potential (**JK-55**: 1.02 V *vs.* NHE; **JK-56**: 1.05 V *vs.* NHE) is higher than that of the iodide electron donor providing a thermodynamic driving force for efficient dye regeneration. The excited-state redox potentials, $\Phi^{\circ}(S^{+}/S^{*})$, of **JK-55** and **JK-56** calculated from the redox potential and emission spectrum are calculated to be −0.87 and −0.96 V *vs.* NHE, respectively, which is more negative than the conduction band edge of TiO_2 (−0.5 V *vs.* NHE), providing the driving force for electron injection.

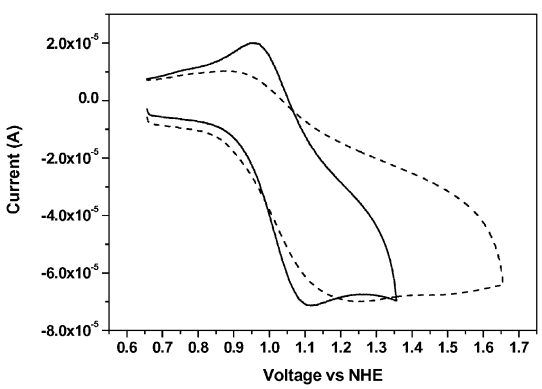

Fig. 3 CV of **JK-55** (—) and **JK-56** (--) on TiO_2 with 0.1 M $(n\text{-}C_4H_9)_4NPF_6$ acetonitrile solution (scan rate of 50 mV s^{-1}).

The photovoltaic performances of the **JK-55**, **JK-56** and **N719** sensitized cells are presented in Table 1. Under standard global AM 1.5 solar condition, the short-circuit photocurrent density (J_{sc}), open-circuit voltage (V_{oc}) and fill factor (*ff*) of the device with the **JK-56** sensitizer are 17.48 mA cm^{-2}, 0.71 V and 0.73, respectively, corresponding to an overall conversion efficiency of 9.16%. The **JK-55** sensitized solar cell yields comparable short-circuit photocurrent density and fill factor but the V_{oc} is lower than that of **JK-56** sensitizer (see Table 1). The V_{oc} enhancement of **JK-56** compared to **JK-55** can be correlated with the decrease of dark current due to the increased amount of dye on TiO_2. To clarify the above explanation, we have measured the amount of dyes absorbed on a 10 μm TiO_2 film by desorbing from the surface. The absorbed amounts of 4.98×10^{-9} mol cm^{-2} for **JK-55** and 3.47×10^{-8} mol cm^{-2} for **JK-56** are observed. The low adsorption of **JK-55** can be due to the presence of two bulky organic groups.

The photocurrent action spectra of the three sensitizers are presented in the inset of Fig. 4. The incident photon to current conversion efficiency (IPCE) of **JK-56** exhibits a high plateau in a broad spectral range from 450 to 600 nm, reaching a maximum of 83% at 550 nm. The increase of the IPCE of **JK-56** below 480 nm compared to **N719** is caused by the presence of organic sensitizer, leading to a slight increase in the current and of an overall conversion efficiency (η).

Electron transport in DSSCs can be characterized by two major parameters; electron diffusion coefficient (D_e) and electron lifetime (τ_e). D_e was derived by a time constant (τ_c) determined by fitting the decay of the photocurrent transients with a single exponential and the TiO_2 film thickness by $D_e = w^2/2.77\tau_c$ (here, w is the film thickness). Moreover, τ_e is the parameter related to the electron recombination. This parameter can also be determined by fitting the decay of the photovoltage transients with a single exponential (*i.e.* $\exp(-t/\tau_e)$).[8]

Fig. 5 shows the D_e (a) and τ_e (b) values *vs.* short-circuit currents in the photoanodes adsorbing different dyes (*i.e.* **N719**, **JK-55** and **JK-56**). The J_{sc} values in the *x*-axis increased with an increase in the initial laser intensity controlled by ND filters with different optical densities. The D_e values of the photoanodes adsorbing the **JK-55** and **JK-56** dyes are shown to be very similar to those of **N719** at identical short-circuit current conditions. Meanwhile, the difference in the τ_e values was a result of the different amount of dyes absorbed on TiO_2. The absorbed dye amount decreased with an increase in the molecular size of the dyes. It is believed that the electron recombination occurred more significantly in the photoelectrodes adsorbing the dyes with more bulky structure owing to the relatively large TiO_2 surface area unoccupied by dye molecules. The result of the electron lifetime is well consistent with that of V_{oc} shown in Table 1.

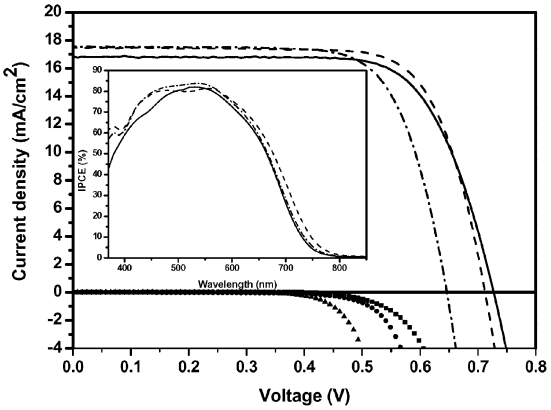

Fig. 4 *J–V* curve and IPCE spectra of **N719** (—), **JK-55** (--) and **JK-56** (---). Dark current spectra of **N719** (■), **JK-55** (●) and **JK-56** (▲).

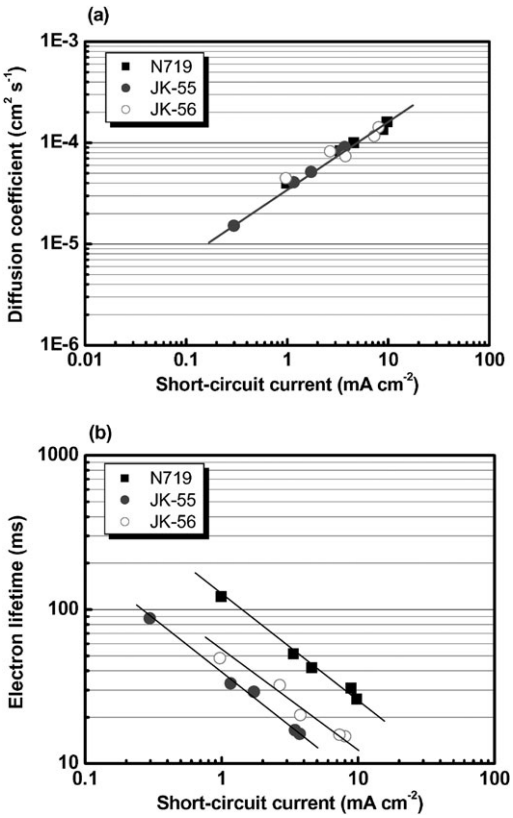

Fig. 5 Electron diffusion coefficients (a) and lifetimes (b) in the photoelectrodes adsorbing different dyes (**N719**, **JK-55**, and **JK-56**).

Table 1 Optical, redox and DSSC performance parameters of dyes

Dye	λ_{abs}[a]/nm (ε/M^{-1} cm^{-1})	E_{redox}[b](ΔE_p)/V	E_{0-0}[c]/V	E_{LUMO}[d]/V	J_{sc}/mA cm^{-2}	V_{oc}/V	FF	η[e] (%)
JK-55	354 (58 600), 470 (38 800), 539(22 800)	1.02	1.89	−0.87	17.55	0.64	0.72	8.20
JK-56	352 (35 900), 463 (24 400), 537 (18 400)	1.05	2.01	−0.96	17.48	0.71	0.73	9.16
N719	535 (14 700)				16.85	0.73	0.72	8.85

[a] Absorption spectra were measured in DMF. [b] Redox potential of dyes on TiO_2 were measured in CH_3CN with 0.1 M (n-$C_4H_9)_4NPF_6$ with a scan rate of 50 mV s^{-1} (*vs.* NHE). [c] E_{0-0} was determined from intersection of absorption and emission spectra in ethanol. [d] E_{LUMO} was calculated by E_{ox}–E_{0-0}. [e] Performances of DSSCs were measured with 0.18 cm^2 working area.

Conclusions

We have meticulously engineered at the molecular level to incorporate an organic antenna moiety into a ruthenium sensitizer that not only enhances significantly the molar extinction coefficient but also the panchromatic response of the sensitizer, yielding 83% IPCE and 9.16% power conversion efficiency, under AM 1.5 solar condition. Also the bis-dimethylfuluorenyl amino benzo[*b*]thiophene secondary electron-donor group employed in this study can be expected to increase the distance between the surface and the hole, resulting in an long-lived charge-separated pair.

Experimental

All reactions were carried out under an argon atmosphere. Solvents were distilled from appropriate reagents. All reagents were purchased from Sigma-Aldrich. 6-(bis(9,9-dimethylfluoren-2-yl)amino)-2-formylbenzothiophene (**1**)[4] and 4,4′-bis(diethylphosphonomethyl)-2,2′-bipyridine (**2**) and 4-(diethylphosphonomethyl)-4′-methyl-2,2′-bipyridine (**3**)[5] were synthesized using a modified procedure of previous references. ^{1}H and ^{13}C NMR spectra were recorded on a Varian Mercury 300 spectrometer. Elemental analyses were performed with a Carlo Elba Instruments CHNS-O EA 1108 analyzer. Mass spectra were recorded on a JEOL JMS-SX102A instrument. The absorption and photoluminescence spectra were recorded on a Perkin-Elmer Lambda 2S UV-visible spectrometer and a Perkin LS fluorescence spectrometer, respectively.

Three sensitizers, **JK-55**, **JK-56** and **N719**, have been used to fabricate solar cells to explore the photovoltaic performance using 10 + 4 μm TiO_2 layers. The first layer of 10 μm thickness was prepared by doctor blade printing TiO_2 paste (Solaronix, Ti-Nanoxide T/SP), and the second TiO_2 scattering layer of 4 μm thickness was coated with 400 nm anatase particles (CCIC, PST-400C). The double layer film was treated with 40 mM $TiCl_4$ solution as reported by the Grätzel group.[7] The resulting layer was sintered at 500 °C for 30 min. After cooling to 70 °C, the films were immersed into the **JK-55**, **JK-56** and **N719** solutions (0.3 mM DMF containing 10 mM 3a,7a-dihydroxy-5b-cholic acid). The stained TiO_2 electrode and Pt-counter electrode were assembled into a sealed sandwich-type cell by heating at 80 °C with a hot-melt ionomer film as a spacer between the electrode. The electrolyte was composed of 0.6 M DMPImI, 0.05 M I_2, 0.1 M LiI and 0.5 M *tert*-butylpyridine in acetonitrile.

Cyclic voltammetry was carried out with a BAS 100B (Bioanalytical Systems, Inc.). A three-electrode system was used and consisted of a gold disk, working electrode and a platinum wire electrode. Redox potentials of dyes on TiO_2 were measured in CH_3CN with 0.1 M $(n\text{-}C_4H_9)_4NPF_6$ at a scan rate of 50 mV s^{-1} (*vs.* Fc/Fc^+).

Syntheses

4,4′-Di{bis[(9,9-dimethylfluoren-2-yl)amino]-2-benzo[*b*]-thiophenylvinylene}-2,2′-bipyridine (4). Potassium *tert*-butoxide (0.09 g, 0.801 mmol) was added to a solution of 6-(bis(9,9-dimethylfluoren-2-yl)amino)-2-formylbenzo[*b*]thiophene (0.3 g, 0.534 mmol) and 4,4′-bis(diethylphosphonomethyl)-2,2′-bipyridine (0.12 g, 0.267 mmol) in THF (30 mL). The reaction mixture was stirred for 10 h at room temperature. After addition of water (10 mL), THF was removed under reduced pressure, and the aqueous residue was extracted with CH_2Cl_2 (50 mL). The collected organic layer was washed with water (50 mL), dried over magnesium sulfate, and filtered. The solvent was removed under reduced pressure. The pure product **4** was obtained by silica gel chromatography (eluent ethyl acetate–hexane = 1 : 1, R_f = 0.3) to afford **4** in 51% yield; mp 194 °C. ^{1}H NMR ($CDCl_3$): δ 8.67 (d, J = 5.1 Hz, 2H), 8.54 (s, 2H), 7.74–7.61 (m, 10H), 7.57 (s, 2H), 7.39–7.25 (m, 22H), 7.20 (d, J = 5.1 Hz, 2H), 7.13 (m, d, J = 7.8 Hz, 4H), 6.92 (d, J = 15.0 Hz, 2H), 1.41 (s, 24H). ^{13}C{^{1}H} NMR ($CDCl_3$): δ 156.5, 155.3, 153.7, 149.7, 147.4, 146.3, 145.3, 141.0, 140.6, 139.0, 138.5, 137.4, 135.5, 134.5, 128.4, 127.1, 126.7, 125.3, 124.4, 123.4, 122.6, 121.5, 120.8, 119.6, 118.8, 118.0, 116.9, 47.0, 27.2. MS: m/z 1270 [M^+]. Anal. Calc. for $C_{90}H_{70}N_4S_2$: C, 85.00; H, 5.55. Found: C, 84.76; H, 5.12%.

4-Methyl-4′-bis[(9,9-dimethylfluoren-2-yl)amino]-2-benzo[*b*]-thiophenylvinylene-2,2′-bipyridine (5). Compound **5** was synthesized by a procedure to **4** except that 4-(diethylphosphonomethyl)-4′-methyl-2,2′-bipyridine (0.27 g, 0.854 mmol) was used in place of 4,4′-bis(diethylphosphonomethyl)-2,2′-bipyridine; yield 61%; mp 197 °C. ^{1}H NMR ($CDCl_3$): δ 8.63 (d, J = 4.8 Hz, 1H), 8.57 (d, J = 4.2 Hz, 1H), 8.51 (s, 1H), 8.27 (s, 1H), 7.67–7.60 (m, 6H), 7.57 (s, 1H), 7.41–7.21 (m, 10H), 7.20 (d, J = 4.8 Hz, 1H), 7.14 (d, J = 4.2 Hz, 1H), 7.12 (d, J = 8.1 Hz, 2H), 6.90 (d, J = 15.6 Hz, 1H), 2.45 (s, 3H), 1.42 (s, 12H). ^{13}C{^{1}H} NMR ($CDCl_3$): δ 156.7, 156.6, 155.9, 155.3, 153.7, 149.6, 149.0, 148.4, 147.4, 146.3, 145.3, 140.9, 140.6, 139.0, 135.5, 134.5, 127.1, 127.0, 126.7, 125.3, 124.9, 124.4, 123.4, 122.6, 122.4, 122.2, 121.0, 120.8, 119.6, 118.8, 118.0, 116.9, 47.0, 27.1, 21.3. MS: m/z 727 [M^+]. Anal. Calc. for $C_{51}H_{41}N_3S$: C, 84.15; H, 5.68. Found: C, 83.87; H, 5.24%.

JK-55. **4** (0.15 g, 0.118 mmol) and dichloro(*p*-cymene)ruthenium(II) dimer (0.036 g, 0.058 mmol) in DMF were heated at 80 °C for 4 h under argon in the dark. Subsequently, 4,4′-dicarboxylic acid-2,2′-bipyridine (0.029 g, 0.118 mmol) was added and the reaction mixture was heated to 160 °C for another 4 h. To the resulting dark green solution was added solid NH_4NCS (0.076 g, 1 mmol) and the reaction mixture was further heated for 4 h at 130 °C. DMF was removed on a rotary evaporator under vacuum and water (200 ml) was added to induce precipitation. The purple solid was filtered off, washed with water and Et_2O, and dried under vacuum. The crude compound was dissolved in basic methanol (with TBAOH) and further purified on the Sephadex LH-20 with methanol as eluent. The main band was collected, concentrated and precipitated with acidic methanol (HNO_3) to obtain pure **JK-55** in 48% yield. ^{1}H NMR (DMSO-d_6): δ 9.40 (d, 1H), 9.16 (d, 1H), 9.02 (s, 1H), 8.99 (s, 1H), 8.86 (d, J = 5.1 Hz, 2H), 8.74 (s, 2H), 8.57 (d, J_{HH} = 5.1 Hz, 1H), 8.51 (d, J = 5.1 Hz, 1H), 7.84–7.73 (m, 10H), 7.67 (s, 2H), 7.59–7.47 (m, 22H), 7.40 (d, J = 5.1 Hz, 2H), 7.24 (m, d, J = 7.8 Hz, 4H), 7.12 (d, J = 15.0 Hz, 2H), 1.36 (s, 24H). Anal. Calc. for

$C_{104}H_{78}N_8O_4RuS_4$: C, 72.07; H, 4.54. Found: C, 71.56; H, 4.04%.

JK-56. JK-56 was synthesized by the same procedure as **JK-55** except that compound **5** (0.25 g, 0.343 mmol) was used in place of compound **4**; yield: 51%. ^{1}H NMR (DMSO-d_6): δ 9.40 (d, 1H), 9.16 (d, 1H), 9.02 (s, 1H), 8.99 (s, 1H), 8.57 (d, $^3J_{HH}$ = 5.1 Hz, 1H), 8.51 (d, J = 5.1 Hz, 1H), 8.83 (d, J = 4.8 Hz, 1H), 8.76 (d, J = 4.2 Hz, 1H), 8.71 (s, 1H), 8.45 (s, 1H), 7.86–7.75 (m, 6H), 7.68 (s, 1H), 7.52–7.41 (m, 10H), 7.40 (d, J = 4.8 Hz, 1H), 7.36 (d, J = 4.2 Hz, 1H), 7.32 (d, J = 8.1 Hz, 2H), 7.10 (d, J = 15.6 Hz, 1H), 2.41 (s, 3H), 1.37 (s, 12H). Anal. Calc. for $C_{65}H_{49}N_7O_4RuS_3$: C, 65.64; H, 4.15. Found: C, 65.12; H, 3.87%.

Computational method

Our total energy calculations are performed using the Vienna *ab initio* simulation program (VASP).[9] Electron–ion interaction is described by the projected augmented wave (PAW) method.[10] Exchange–correlation effect is treated within the local density approximation. We adopt a supercell geometry in which k-space sampling is done with Γ-points. In doing this, we use large supercells which guarantee interatomic distances between neighboring cells along each direction greater than 10.0 Å. Cut-off energy (= 300 eV) is set high enough to guarantee accurate results. In regard to this, we wish to point out that the PAW calculation does not rely on a localized orbital basis but on the plane wave basis. The conjugate gradient method is employed to optimize the geometry until the Hellmann–Feynman force exerted on an atom is less than 0.03 eV Å^{-1}. Reliability of the calculation within the PAW was confirmed in our recent calculations on the electronic and chemical properties of various systems ranging from organometallic systems to nanotubes.[11]

Acknowledgements

We are grateful to the Korea Science and Engineering Foundation (KOSEF) through the National Research Lab. Program funded by the Ministry of Science and Technology (No. R0A-2005-000-10034-0) and BK-21 (2006). We also appreciate Jeonju University for financial support.

References

1 (*a*) B. O'Regan and M. Grätzel, *Nature*, 1991, **353**, 737; (*b*) M. Grätzel, *Nature*, 2001, **414**, 338.
2 (*a*) M. Grätzel, *J. Photochem. Photobiol. C*, 2003, **4**, 145; (*b*) M. K. Nazeeruddin, F. De Angelis, S. Fantacci, A. Selloni, G. Viscardi, P. Liska, S. Ito, T. Bessho and M. Grätzel, *J. Am. Chem. Soc.*, 2005, **127**, 16835; (*c*) M. Grätzel, *Prog. Photovolt. Res. Appl.*, 2006, **14**, 429.
3 (*a*) R. Amadelli, R. Argazzi, C. A. Bignozzi and F. Scandola, *J. Am. Chem. Soc.*, 1990, **112**, 7099; (*b*) A. F. Nogueira, S. H. Toma, M. Vidotti, A. L. B. Formiga, S. I. C. De Torresi and H. E. Toma, *New J. Chem.*, 2005, **29**, 320; (*c*) S.-R. Jang, R. Vittal, J. Lee, N. Jeong and K.-J. Kang, *Chem. Commun.*, 2006, 103.
4 (*a*) S. Kim, J. K. Lee, S. O. Kang, J. Ko, J.-H. Yum, S. Fantacci, F. D. Angelis, D. D. Censo, M. K. Nazeeruddin and M. Grätzel, *J. Am. Chem. Soc.*, 2006, **128**, 16701; (*b*) H. Choi, C. Baik, S. O. Kang, J. Ko, M.-S. Kang, M. K. Nazeeruddin and M. Grätzel, *Angew. Chem., Int. Ed.*, 2008, **47**, 327; (*c*) H. Choi, J. K. Lee, K. Song, S. O. Kang and J. Ko, *Tetrahedron*, 2007, **63**, 3115.
5 (*a*) C. Zhang, A. W. Harper and L. R. Dalton, *Synth. Commun.*, 2001, **31**, 1361; (*b*) S. Jang, C. Lee, H. Choi, J. Ko, J. Lee, R. Vittal and K. Kim, *Chem. Mater.*, 2006, **18**, 5604.
6 P. Wang, S. M. Zakeeruddin, J. E. Moser, M. K. Nazeeruddin, T. Sekiguchi and M. Grätzel, *Nat. Mater.*, 2003, **2**, 402.
7 M. K. Nazeeruddin, A. Kay, I. Rodicio, R. Humphry-Baker, E. Müller, P. Liska, N. Vlachopoulos and M. Grätzel, *J. Am. Chem. Soc.*, 1993, **115**, 6382.
8 (*a*) S. Nakade, T. Kanzaki, Y. Wada and S. Yanagida, *Langmuir*, 2005, **21**, 10803; (*b*) K. S. Ahn, M.-S. Kang, J. K. Lee, B. C. Shin and J. W. Lee, *Appl. Phys. Lett.*, 2006, **89**, 013103; (*c*) K.-S. Ahn, M.-S. Kang, J. W. Lee and Y. S. Kang, *J. Appl. Phys.*, 2007, **101**, 084312.
9 (*a*) G. Kresse and J. Hafner, *Phys. Rev. B*, 1993, **47**, RC558; (*b*) G. Kresse and J. Furthmuller, *Phys. Rev. B*, 1996, **54**, 11169.
10 G. Kresse and D. Joubert, *Phys. Rev. B*, 1999, **59**, 1758.
11 For example, see S. Y. Kim, J. Park, H. C. Choi, J. P. Ahn, J. Q. Hou and H. S. Kang, *J. Am. Chem. Soc.*, 2007, **129**, 1705, and references therein.